THE OHIO STATE UNIVERSITY

UNDERGRADUATE RESEARCH DISTINCTION THESIS

Development of Oxygen-Sensitive Electrosprayed Core-shell Polymer Microparticles for Biological Applications

---

Author:
Nicole DIRANDO

Supervisor:
Dr. John LANNUTTI

A thesis submitted in fulfillment of the requirements
for the undergraduate research distinction in the

Department of Materials Science and Engineering

April 13, 2018

THE OHIO STATE UNIVERSITY

Abstract

Dr. John Lannutti

Department of Materials Science and Engineering

Research Distinction

Development of Oxygen-Sensitive Electrosprayed Core-shell Polymer Microparticles for Biological Applications

by Nicole DiRANDO

When upconverting nanoparticles (UCNPs) are combined with oxygen-sensitive molecules, oxygen sensing can be achieved upon near-infrared (NIR) excitation. The combination of the oxygen-sensitive molecules and upconverters can be used to show different oxygen concentrations in the body. If there is a large concentration of oxygen, the intensity of the light emitted will be lower compared to if there were less oxygen. The objective of this research is to develop optimal electrosprayed microparticles and to better understand their polymer processing in order to achieve desired properties. Ideally, the particles will result in high brightness and low leaching. The developed microparticles can provide a useful benefit to biological applications such as locating hypoxic regions in tumors.

Acknowledgements

I would like to thank my research adviser, Dr. John Lannutti, for allowing me to expand my knowledge in the area of electrospraying polymer particles and to Kayla Presley for assisting me in various procedures and tasks to further my research progress. Lastly I would like to thank Dr. Carlos Castro (Department of Mechanical and Aerospace Engineering) for taking his time out of his busy schedule to participate in my oral defense.

Contents

Abstract **i**

Acknowledgements **ii**

List of Abbreviations **vii**

1 Introduction **1**

1.1 Background and Motivation 1

1.2 Significance of Research 3

1.3 Overview of Thesis 4

2 Methodology **5**

2.1 Microparticle Polymer Processing 5

2.1.1 Electrospraying 5

2.1.2 Materials 6

2.1.3 Preparation of Polymer Core-Shell Micorparticles 6

2.2 Processing Treatments 7

2.2.1 Pre-Processing Treatments 7

2.2.2 Post-Processing Treatments 8

2.3 Experimentation 9

2.3.1 Parameters 9

2.3.2 Leaching Profile 11

2.4 Analysis Methods 13

3 Results **15**

3.1 Microparticles 15

3.1.1 Morphology 15
3.1.2 Measurements - Size, Diameter, and Pore Distribution 18
3.1.3 Agglomeration 21
3.2 Leaching Design of Experiments 23
3.2.1 Percent Released 23
3.2.2 JMP Statistical Analysis 26

4 Discussion **28**
4.1 Conclusion 28
4.2 Contribution 30
4.3 Future Work 31

A Design of Experiments for Leaching Study **32**

List of Figures

1.1 Electropsrayed Particles at Various Oxygen Concentrations 2

2.1 Core-Shell Electrospraying Diagram 7

3.1 Increased Polymer Weight Leading to Fiber Formation 15
3.2 Comparison of Various Solvent Ratios 16
3.3 Formulation A Core-Shell Flow Rates at 20 cm Collection Distance 18
3.4 Formulation A Microparticles at Various Distances 19
3.5 Area of Pores on Microparticle Shell Surface 20
3.6 Comparison of Particles with and without Dispersing Agent 22
3.7 Sonicated Versus Unsonicated Sample 22
3.8 Amount Released (mg) Versus Sample Type 23
3.9 Percent Released (%) Versus Sample Type 24
3.10 $Ru(dpp)_3Cl_2$ Released in PBS and Water 25
3.11 Day 1 ANOVA Statistics 26
3.12 Day 1 LSMeans Differences Student's t Solvent Ratio 27
3.13 Day 1 LSMeans Differences Student's t Solvent Ratio*Flow Rate 27

A.1 Day 2 ANOVA Statistics 32
A.2 Day 7 ANOVA Statistics 33
A.3 Day 10 ANOVA Statistics 33
A.4 Day 14 ANOVA Statistics 34

List of Tables

2.1 Polymer Concentration and Solvent Ratio Formulations 10
2.2 Polymer Solution Flow Rates and Collection Distances 11
2.3 2^2-Factorial Design of Experiments with 3 Replicates 12
2.4 Leaching Experiment Formulations 13

List of Abbreviations

NIR	**N**ear **I**nfrared
SEM	**S**canning **E**lectron **M**icroscope
TIRF	**T**otal **I**nternal **R**eflection **F**luorescence
UCNPs	**U**pconverting **N**anoparticles
DCM	**D**ichoromethane
HFP	1,1,1,3,3,3-**H**exafluoro-2-propanol
PSU	**P**olysulfone
$Ru(dpp)_3Cl_2$	Tris(4,7 -diphenyl-1, 10-phenanthroline)ruthenium(II) dichloride
ePTFE	**e**xpanded **P**olytetrafluoroethylene

1 Introduction

1.1 Background and Motivation

The development of near infrared oxygen sensitive core-shell polymer microparticles can provide beneficial advantages to biological applications. Luminescent oxygen-sensing molecules show great promise for biological applications, but are typically incorporated into thin films. However, non-linear Stern Volmer plots are generally achieved, and the response time of these sensor films can be quite slow. [17] However, research from Dr. Lannutti's lab and others has incorporated these molecules into electrospun scaffolds. The increased surface-to-volume ratio, small diameters, and porosity leads to a greatly reduced response time. Additionally, the rapid solvent evaporation allows for a linear Stern-Volmer plot. [15] Equation 1.1 below represents the Stern-Volmer equation which is described as the relative intensity change as a function of oxygen concentration.

$$I_0 / I = 1 + K_{SV}[O_2] \tag{1.1}$$

Where K_{SV} is the Stern-Volmer quenching constant

The equation should follow a linear relationship, where the relative intensity change (I_0 / I) is directly proportional to the change in oxygen ($[O_2]$). [15]

More recently, the lab has been interested in extending this to biological applications where tissue penetration is a limiting factor. Luminescent oxygen sensors typically require violet or blue excitation, which does not penetrate tissue deeply because of high levels of absorption and scattering through the tissue layers. A solution to this barrier is the use of upconverting nanoparticles (UCNPs) in combination with the oxygen-sensitive molecule, $Ru(dpp)_3Cl_2$. [2] This strategy allows a deeper penetration through the tissue while maintaining minimal damage. The upconverters demonstrate

a multi-photon process, where they absorb higher wavelength photons (980 nm) and emit shorter ones (480 nm blue light). [11] When using 980 nm near-infrared light to excite the upconverters, the blue emission would locally trigger an oxygen-sensitive molecule to emit a red phosphorescence (625 nm). Due to a transfer in energy, the red phosphorescence would be quenched relative to the amount of oxygen present in the region. [1]

However, these nanofibers are not injectable. Since an injectable form is desired, an electrospraying process has been adapted. As with the fiber scaffolds, previous experimentation within Dr. Lannutti's lab has demonstrated the oxygen sensing capabilities of these electrosprayed microparticles. Figure 1.1 shows a sample of electrosprayed mi-

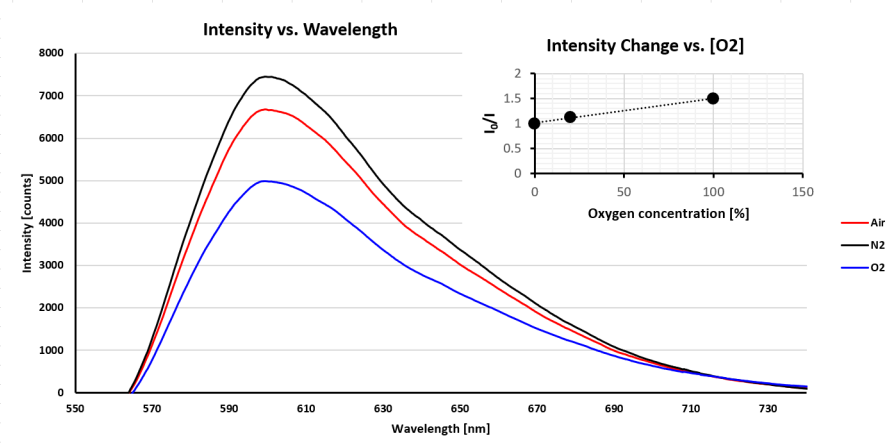

FIGURE 1.1: Electropsrayed Particles at Various Oxygen Concentrations

croparticles being exposed to various levels of oxygen concentration. When exposed to pure N_2 the intensity of the fluorescent output is greatest. Once exposed to pure O_2 the intensity decreases, as expected due to the output being quenched by the presence of oxygen. The small diagram in the upper right corner depicts the corresponding Stern-Volmer plot for this data. As expected, there is a linear relationship between the change in intensity versus oxygen concentration; validating that electrosprayed microparticles provide a useful advantage to oxygen sensing capabilities.

Electrospraying is a technique of converting a polymer solution into fine droplets by administering electrical forces. A syringe pump will be set to a given flow rate where the polymer solution will be ejected out of the needle tip and electrically charged. The

electrical force, applied at the needle tip, quickly evaporates the solvent in the solution and the microparticles are attracted to a grounded metal collecting plate below. [6] It is desired to achieve the same oxygen sensing capabilities as the polymer fiber scaffolds, such as fast-response time and linear Stern-Volmer plot. In order for that to occur, the microparticles must have optimal core-shell morphology and dispersion to achieve the ideal combination of high brightness and low leaching. Also, they must have proper incorporation of the UCNPs in order for transmitting light to penetrate through tissue.

A solid core-shell method has been adopted in order to produce these microparticles. The main reason the lab has adopted the core-shell technique is because it is undesirable to leach the $Ru(dpp)_3Cl_2$ dye due to its toxicity to cells. The dye and UCNPs reside in the solid core; while solid polymer is in a shell exterior. Typically a liquid core is used for controlled drug release applications [3], but a solid core has been developed because the oxygen sensing dye tends to self-quench and has to be distributed in some sort of matrix.

There is a multitude of biological applications where it is important to know the oxygen concentration. [11] Since the development of these microparticles are intended for injectable usage within the body, light penetrating through the tissue becomes an issue and leaching of dye poses the threat of toxicity to cells. If the optimal core-shell microparticles are developed they will be able to address these injectability issues and provide useful advantages to biological applications; in particular hypoxic regions in tumors.

1.2 Significance of Research

It is necessary that the most optimal microparticles are developed in order to try and achieve the desired properties comparable to the electrospun fiber scaffolds. The co-axial electrospraying process is a relatively emerging technology; only being around

since 2002. There lacks a significant amount of literature providing reliable and reproducible methods of fabrication of these microparticles; especially when a polymer-polymer core-shell matrix is desired. Thus, it is important and necessary to design processing guidelines in order to produce electrosprayed particles in broader research areas. [16]

Like previously mentioned, this research can provide significant advantages to the biomedical field. It is known that hypoxic areas are better at resisting cancer treatment, such as radiation and chemotherapy; it is desired to be able to locate those regions. [8, 14] This research provides a method and guidelines to produce the best injectable form of microparticles that, upon NIR excitation, can provide a useful application to the monitoring of oxygen and identification of hypoxic regions of tumors. [2]

1.3 Overview of Thesis

There are two main goals of this research: (1) identify several promising processing parameters of the electrosprayed microparticles in an attempt to achieve properly dispersed, dense, and spherical morphologies (2) Analyze said processing parameters to define processing guidelines in an attempt to develop reproducible microparticles.

The first goal revolved around altering various processing parameters such as collection distance, flow rates, and solutions. Pre- and post-processing parameters were determined and incorporated into the method of fabrication. Morphology and agglomeration of sample solutions were then analyzed. Once the optimal processing parameters were evaluated and the various morphology characterization was observed; a leaching design of experiments was conducted to observe trends of dye diffusion from the core of the polymer microparticles. This data could potentially provide validation that the various morphologies observed (i.e. a porous shell) could be incorporated into a drug release application. Using the information and parameters obtained from goal (1), guidelines were suggested that could be used for future work and experimentation involving the injectibility and incorporation of the UCNPs.

2 Methodology

2.1 Microparticle Polymer Processing

2.1.1 Electrospraying

The polymer core-shell microparticles are developed through an electrospraying process. Simply put, a polymer solution is loaded into a syringe that is ejected at a specific flow rate via a syringe pump while a capillary, such as a needle tip, is electrically charged. Electrospraying uses the method known as electrohydrodynamic atomization; producing solid microparticles by applying an electric field to a liquid droplet exiting a capillary by forming the *Taylor Cone*. [3] The *Taylor Cone* is a phenomenon that results from an electrically conductive liquid exposed to a strong vertical electric field. The free surface of the liquid gains a surface charge; allowing the liquid to form the cone. [9] When a proper *Taylor Cone* is formed tiny particles spray off the jet, the solvent evaporates, and the particles can be collected on a grounded plate.

Various parameters, such as flow rate, collection distance, and polymer solution, can have an influence on the microparticle morphology. For example, polymer concentration can effect the morphology of the microparticles due to chain entanglements. With higher polymer concentrations there exhibits greater chain entanglement; resulting in fiber formation during the electropsraying process. The solvent ratio can also lead to various surface morphology differences among microparticles. When a two-solvent ratio is introduced into the polymer mixture, the solvent with the lower boiling point will be removed faster; thus leaving the higher boiling point solvent enriched in the solution. When the liquid solution is electrically charged as it exits the capillary the solvent evaporates. [10] Depending on the phase separation, porous structures may appear on the surface of the microparticles or fiber tails. The distance between the collection plate

and needle tip has shown in previous studies to have an influence on particle size. The distance between the grounded plate and needle allows for solvent evaporation to occur. If the distance between the ground and needle is increased, this allows for longer evaporation time but results in a decrease of electric potential. It the evaporation time is too short, the particles will not have enough time to dry and remain as droplets or form a film. [10] Lastly, it has been demonstrated through previous studies that flow rate of the polymer solution can influence the microparticle size distribution. When the flow rate of the syringe pump is increased, more solution is driven out of the needle tip; thus influencing the diameter of the particle droplets. [12]

2.1.2 Materials

Polysulfone (M_n= 16,000 by MO), Pluronic F-127, Eosin Y (99%) and dichloromethane were purchased from Sigma-Aldrich (St. Louis, MO, USA), and Ruthenium (II) Dichloride was acquired from Alfa Aesar (Ward Hill, MA, USA), and 1,1,1,3,3,3-hexafluoro-2-propanol was obtained from Oakwood Chemical (Estill, SC, USA).

2.1.3 Preparation of Polymer Core-Shell Micorparticles

To prepare the "core" solution, a given wt% of polysulfone was dissolved in a DCM:HFP mixture and $Ru(dpp)_3Cl_2$ was added to the solution with a baseline weight of "X" (versus the weight of PSU), where "X" represents the weight of $Ru(dpp)_3Cl_2$. The "shell" solution consisted of a given wt% of PSU dissolved in a DCM:HFP mixture and Pluronic F-127 added at 1 wt% (versus the weight of PSU). Figure 2.1 depicts the electrospraying process and core-shell setup.

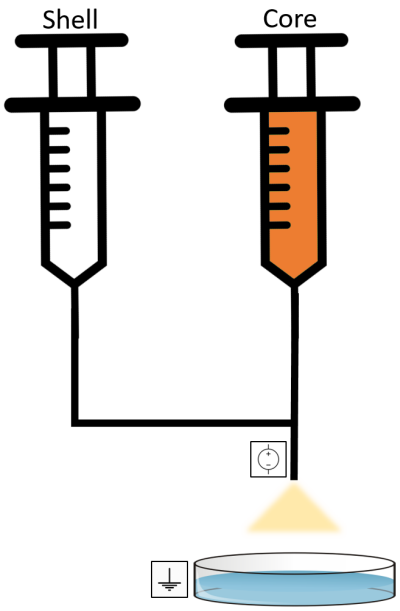

FIGURE 2.1: Core-Shell Electrospraying Diagram

2.2 Processing Treatments

Previous studies in Dr. Lannutti's research group demonstrated microparticle agglomeration when electrosprayed into solution. Once the solution was transferred to the glass vial the microparticles would gravitate towards the sides of the glass vials. This hinders the underlining application for oxygen sensing and decreases the usable yield of particles. This led to multiple investigative studies within this undergraduate thesis to find ways to decrease or rid the microparticles of agglomeration.

2.2.1 Pre-Processing Treatments

Pre-processing treatments such as addition of a dispersing agent and treatment of the glass vials were investigated. Previous shell polymer solutions did not contain any Pluronic F-127, a surfactant. The Pluronic F-127 was introduced into the shell polymer solution with the intention of improving the agglomeration issue. It has been demonstrated in past literature studies that the addition of the Pluronic F-127 surfactant, can

increase efficiencies of electrosprayed fabrication processes. [13] After electrospraying multiple samples and transferring the 15 mL solutions to the glass vials, it was observed that the microparticles would "stick" to the sides of the glass; thus becoming unusable since they would not properly disperse into the solution for the proper concentration. The solution to this issue was to *plasma treat* the glass vials prior to use.

The glass vials underwent the pre-treatment by being exposed to the plasma process for three minutes in order alter the hydrophobic properties of the glass surface. The glass vials were then filled with 15 mL of a 10 wt% Pluronic F-127 and deionized water solution and rested for three hours to allow the surfactant to adhere to the walls. The glass vials were then emptied and washed with a small amount of deionized water. It was expected, based on previous literature, that the plasma treatment would activate and clean the glass surface by contributed to high surface energy with high polarity by removing impurities. [4] This would alter the contact angle between the solution and the glass allowing for different hydrophobic properties.

2.2.2 Post-Processing Treatments

Post-processing treatment was necessary in order to properly disperse the microparticles into the PBS solution. When electrospraying directly into the aluminum dish filled with 15 mL PBS, the microparticles would remain suspended on the top of the liquid and clump together. In order to properly disperse the microparticles into the solution to try and get a uniform concentration, a bath sonication post-treatment process was adopted. A glass vial of the sample was held in a partially filled bath sonicator. Various parameters were tested, such as relaxation and sonication time. The routine that was deemed optimal was as followed: 5 minutes sonication; 60 minutes rest; 5 minutes sonication.

2.3 Experimentation

2.3.1 Parameters

Polymer Formulations

Throughout experimentation, various polymer solutions were made in order to understand the influence of polymer concentration and solvent ratios (by weight) on particle morphology. The polymer formulations are described in Table 2.1. It was hypothesized that the 100% DCM ratio would lead to porous shelled microparticles while an increased HFP ratio would develop fiber tails; due to DCM's lower boiling point and potential phase separation. The samples were electrosprayed at a flow rate ranging between 0.1-0.3 mL/h and 0.5-1.5 mL/h for the core-shell, respectively. They were collected at a distance of either 6.5 cm, 11 cm, 15.5 cm, or 20 cm in an aluminum dish of 15 mL deionized water or PBS for 10 minutes or onto foil. If electrosprayed into an aqueous solution then the samples were transferred to a 15 mL plasma treated glass vial and underwent proper sonication treatment. It should be noted that the core contained 0.5 wt% $Ru(dpp)_3Cl_2$ and the shell contained 1 wt% Pluronic F-127 for all formulations.

TABLE 2.1: Polymer Concentration and Solvent Ratio Formulations

Formulation	Layer	Polymer Concentration (wt%)	DCM Ratio	HFP Ratio
A	Core Shell	1 1	75	25
B	Core Shell	2 1	75	25
C	Core Shell	3 1	75	25
D	Core Shell	1 1	65	35
E	Core Shell	1 1	100	0

Processing Conditions

Other parameters that were altered to observe effect on particle morphology were solution flow rate and collector distance. It was thought that varying the flow rate and collection distance from the needle tip would alter the microparticle diameter. Table 2.2 describes the different parameters and given formulation used for the experiment. It was hypothesized that the shorter collection distances wouldn't allow for proper solvent evaporation and the fast solution flow rates would result in deformation of the microparticle surface. The microparticles were developed by varying the core-shell solution flow rates and collection distance. They were collected in an aluminum dish of 15 mL deionized water for 10 minutes. The particles were then transferred to a 15 mL plasma treated glass vial that was sonicated. As mentioned previously, the core contained 0.5 wt% $Ru(dpp)_3Cl_2$ and the shell 1 wt% Pluronic F-127 for all sample formulations.

TABLE 2.2: Polymer Solution Flow Rates and Collection Distances

Formulation	Layer	Flow Rate (mL/h)	Collection Distance (cm)
A	Core Shell	0.1 0.5	20
A	Core Shell	0.3 0.5	20
A	Core Shell	0.5 0.5	20
A	Core Shell	0.3 1.5	20
A	Core Shell	0.3 1.5	15.5
A	Core Shell	0.3 1.5	11
A	Core Shell	0.3 1.5	6.5

2.3.2 Leaching Profile

Various porous morphology was observed with the 100% DCM solvent ratio (Formulation E) and at different flow rates; thus it was of interest to explore this polymer solution for drug release applications. Since the oxygen sensing dye has the potential to be cytotoxic to cells, it is also of high importance to verify that the core-shell microparticles would not leach said dye when in use (Formulation A). A design of experiments was developed in order to understand the release profile of various microparticle morphologies given certain processing conditions.

A factor screening design was implemented to identify which were the most important factors. The screening design was performed on 2 different factors at 2 levels with 3 replicates. A total of 12 observations were made. This 2 level-factorial design allows for the potential observation of interactions between the different factors. Table 2.3 describes the experimental design.

TABLE 2.3: 2^2-Factorial Design of Experiments with 3 Replicates

Sample	Solvent Ratio	Flow Rate
1	+	+
2	+	-
3	-	+
4	-	-
5	+	+
6	+	-
7	-	+
8	-	-
9	+	+
10	+	-
11	-	+
12	-	-

Level	Flow Rate (mL/h)	Solvent Ratio
+	0.3 core/0.5 shell	75 DCM : 25 HFP
-	0.3 core/0.3 shell	100 DCM

Particles were electrosprayed in accordance to the samples given the possible combination of all the selected levels of the factors. Samples were sprayed at a 20 cm collection distance onto aluminum foil for roughly 1 hour. The microparticles were then scraped off the aluminum foil with a metal spatula and transferred to a 3 cm long ePTFE tube (3 mm diameter) where one end was previously heat sealed. Once roughly 5 mg of the given sample was transferred to the ePTFE tubing, the tubing was heat sealed shut. Heating sealing parameters were as followed: 4 seconds hot; 70 seconds cool using a TTS-8 from Heat Seal Solutions. The loaded tube was then placed in a 2 mL glass vial and filled with 1.5 mL of PBS via a plastic pipette. The samples were placed in an incubator at 37 °C for a period of 2 weeks.

ePTFE tubing was used in order to avoid complications with centrifuging when extracting the liquid for analysis. It was necessary for analysis that no microparticles be transferred when transferring the liquid in order to make sure only the liquid was being analysis for potential dye leaching and not the liquid and dye containing microparticles. It should be noted that samples 1-12 were

made with another fluorescent dye called Eosin Y due to its intermediate molecular weight allowing the dye the potential to leach through the core-shell microparticles so a profile could be observed. The $Ru(dpp)_3Cl_2$ has a much larger molecular weight, making it difficult for the dye to diffuse through the polymer. Since $Ru(dpp)_3Cl_2$ is to be used when performing oxygen sensing analysis, it is not desired to have the dye leach; thus it expected to see an insignificant leaching profile. One $Ru(dpp)_3Cl_2$ sample was made outside of the design of experiments for a "proof of concept" scenario. In order to enhance the fluorescent output for analysis, both dye concentrations were increased. Table 2.4 describes the modified formulations.

TABLE 2.4: Leaching Experiment Formulations

Experiment	Core	Shell
2 Level Factorial	1 wt% PSU + 2 wt% Eosin Y in X DCM : Y HFP[1]	1 wt% PSU + 1 wt% Pluronic F-127 in X DCM : Y HFP[2]
Proof of Concept	1 wt% PSU + 3 wt% Ru(dpp)Cl in 75 DCM : 25 HFP	1 wt% PSU + 1 wt% Pluronic F-127 75 DCM : 25 HFP

[1] Ratio determined by design of experiments, [2] Ratio the same as in core

2.4 Analysis Methods

Scanning Electron Microscope (SEM)

A FEI Nova NanoSEM 400 scanning electron microscope was used at the Campus Microscopy and Imaging Facility. Images were obtained in order to analyze the particle morphology and characteristics such as diameter and pore size. These images were used in Chapter 3 in order to make conclusions based on key findings. SEM samples were prepared either by directly electrospraying

onto foil for a few minutes or taking a drop from a sample solution and letting it dry on the SEM stub.

Fluorescent Microscopy

A fluorescent microscope was used courtesy of Patricia Morris' lab (Department of Material Science and Engineering). The microscope was used to observe the agglomeration of the microparticles in the PBS solution. The pre- and post-processing methods were verified via this analysis technique. Samples were prepared by placing a few drops on a glass microscope slide via a glass pipette. The drops were either allowed to dry prior to analysis or viewed while wet.

Fluorescent Plate Reader

A fluorescent plate reader was used from the Department of Chemistry. The reader was used for the leaching design of experiments. The plate reader read fluorescent output values for the given samples. The system was set in accordance for the absorption and emission of Eosin Y (510 nm, 555 nm respectively) and $Ru(dpp)_3Cl_2$(480 nm, 560 nm respectively). A 96 well plate was used to hold the samples during analyzation. For each sample, 3 replicates were performed with 200 microliters in each well.

3 Results

3.1 Microparticles

3.1.1 Morphology

Particle morphology characteristics, such as a porous shell or fiber tail formation, were studied by varying the solvent ratio and polymer concentrations. It was observed that when the solvent ratio was kept constant at the standard 75:25 ratio and the polymer weight concentration was increased, as in formulations A-C, formation of fiber and fiber-like tails on the microparticles became evident. Figure 3.1 demonstrates the three formulations (A, B, and C) and the formation of fibers.

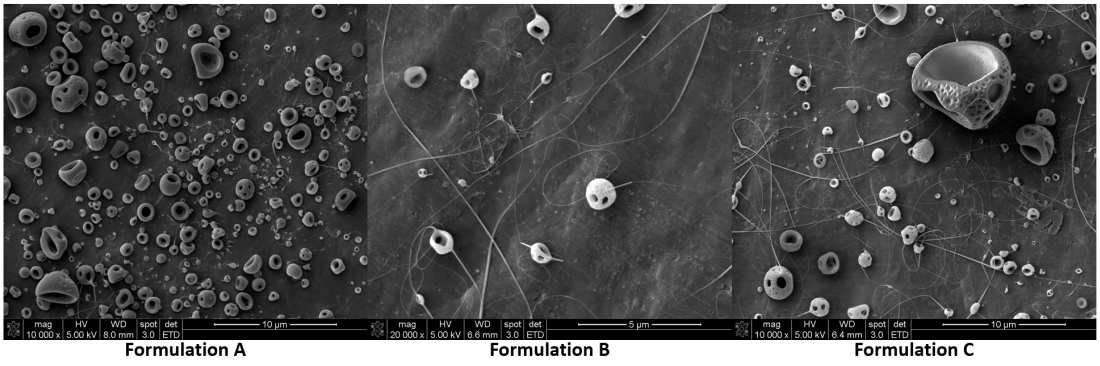

FIGURE 3.1: Increased Polymer Weight Leading to Fiber Formation

The observed fiber formation correlates with previous literature studies. A higher polymer concentration increases the chain entanglement leading to a greater viscosity. [10] If there is too large of a viscosity the *Taylor Cone* can be affected. A larger electric field would become necessary in order to overcome the increased viscosity and form a stable cone. Therefore since the voltage was kept the same for each formulation, Formulations B and C could have had an unstable cone leading to deformed microparticles and formation of fibers.

The solvent ratio was altered in Formulations D and E, keeping the polymer concentration for both the same. They were compared to the baseline ratio in Formulation A. It was observed in Formulation D that the decrease in DCM percentage and increase in HFP lead to fiber formation while the 100% DCM ration in Formulation E led to a porous shell surface. Figure 3.2 demonstrates the observations stated.

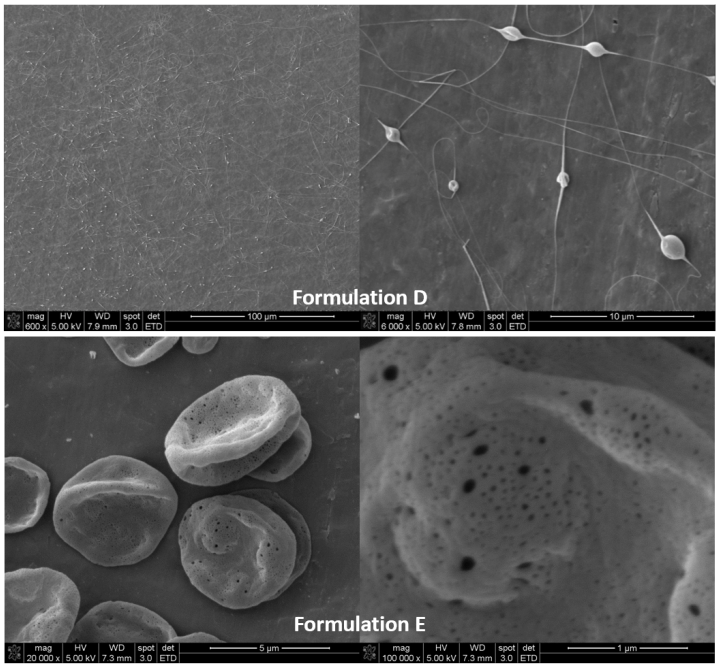

FIGURE 3.2: Comparison of Various Solvent Ratios

As mentioned previously from literature studies, solvent ratios can lead to various surface morphology as shown in Figure 3.2. When there is a two-solvent ratio within the polymer solution, the solvent with the lower boiling point evaporates faster than the higher boiling point solvent. [10] The boiling point of DCM is about 40 °C while HFP has a boiling point of 59 °C; thus it was expected that DCM would evaporate off first leaving HFP as solvent enriched within the solution. [5] In past research from source [10], microparticles that had formulations with lower boiling points resulted in hollow particles; while solvents that had greater boiling points led to smoother and spherical surfaces and particles, respectively. It was observed in the study that with a two solvent mixture that the initial drying rate was similar to the more volatile solvent; while the final rate was similar to the less volatile.

During this study, when the two solvents were in ratio, initially, the DCM would evaporate first, followed by a removal of both DCM/HFP, and in final solvent evaporation the HFP would leave the polymer system. Formulation E contained no HFP and thus DCM would remain solvent enriched the entire time the droplet were to dry. Since it requires less energy to evaporate DCM from the system due to its lower boiling point the DCM was able to evaporate off the particle surface quicker; potentially dissolving some of the polymer shell surface at the same time the particle was drying; thus resulting in pore formation. On the other hand when there is greater amount of HFP in the two solvent system, the microparticles require more energy in order to solidify due to the higher boiling point of HFP. This could cause the microparticles to form the "skin" layer too

slowly hindering the proper formation of the *Taylor Cone* and leading to fiber formation.

3.1.2 Measurements - Size, Diameter, and Pore Distribution

From the parameters in Table 2.2, microparticle size and diameter was studied. It can be observed in Figure 3.3 the various particle size and morphology at a given flow rate and distance.

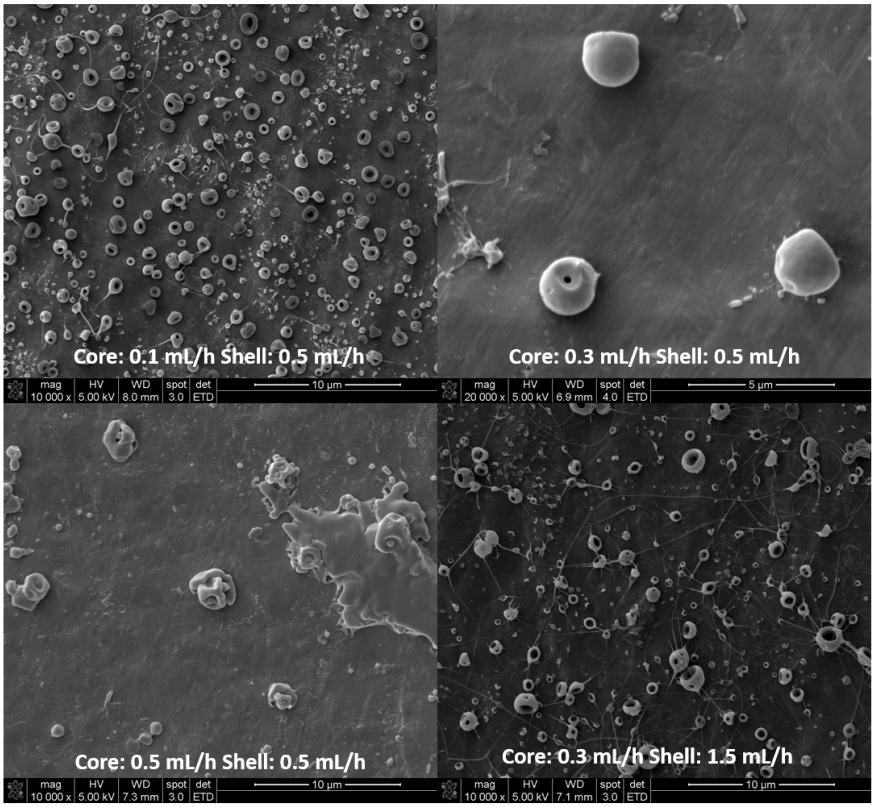

FIGURE 3.3: Formulation A Core-Shell Flow Rates at 20 cm Collection Distance

It was observed that for flow rates of 0.1 mL/h core - 0.5 mL/h shell and 0.3 mL/h core - 0.5 mL/h shell, the microparticle sizes were less than 5 microns; whereas the 0.5 mL/h core - 0.5 mL/h shell and 0.3 mL/h core - 1.5 mL/h shell had microparticles near 5 microns or slightly larger. This correlates with what was demonstrated in past literature studies. [12] Since the first two images operate at slower flow rates less material is being pumped out per hour; resulting in smaller fabricated microparticles.

Observations were also made on the diameter of the microparticles when collection distance became an influencing effect. Figure 3.4 demonstrates the various collection distances and the range of diameters fabricated. It was observed

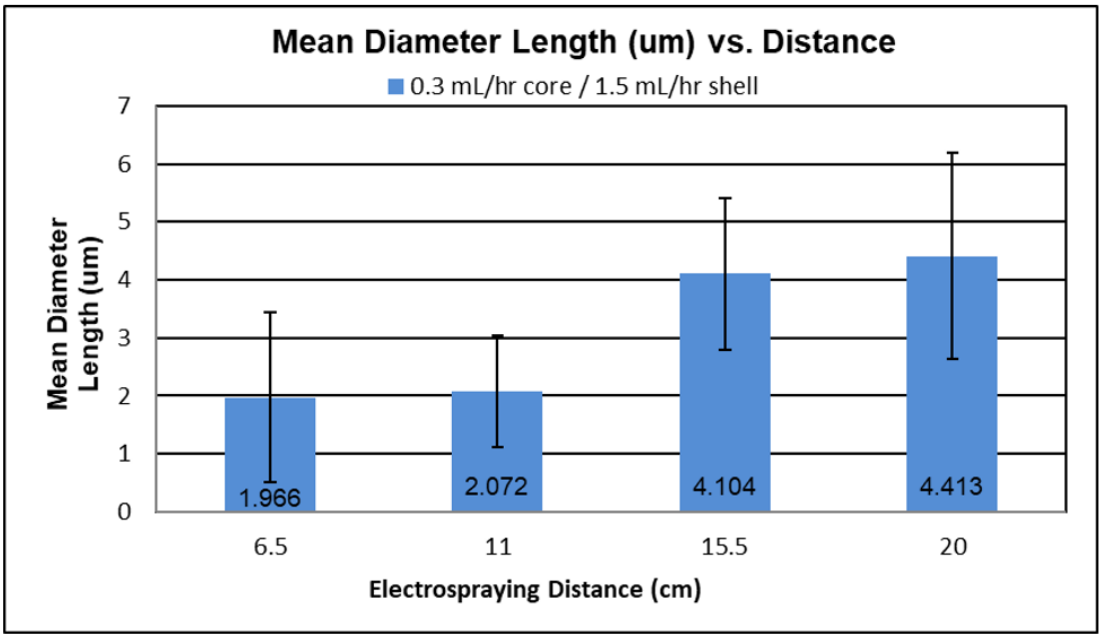

FIGURE 3.4: Formulation A Microparticles at Various Distances

that the microparticles increased in diameter as the electrospraying distances increased. At longer electrospraying distances, the electric potential is decreased. It could be possible that the decrease in potential as the electrospraying distance

increased resulted in particles having more time to form a larger droplet out of the needle tip since the grounding plate was not pulling the polymer solution as strongly as it could have been at the 6.5 cm distance. Another potential factor is that the smaller particles are captured more efficiently at shorter distances and are lost outside the grounded collecting plate at farther distances.

When altering between various flow rates and solvent ratios it was observed that at 100 % (by weight) DCM and alternate core flow rates resulted in different sized surface pores. Using ImageJ Software, pore size distribution for a polymer solution according to Formulation E was measured for a core flow of either 0.3 mL/h or 0.5 mL/h. The results are displayed below in image 3.5.

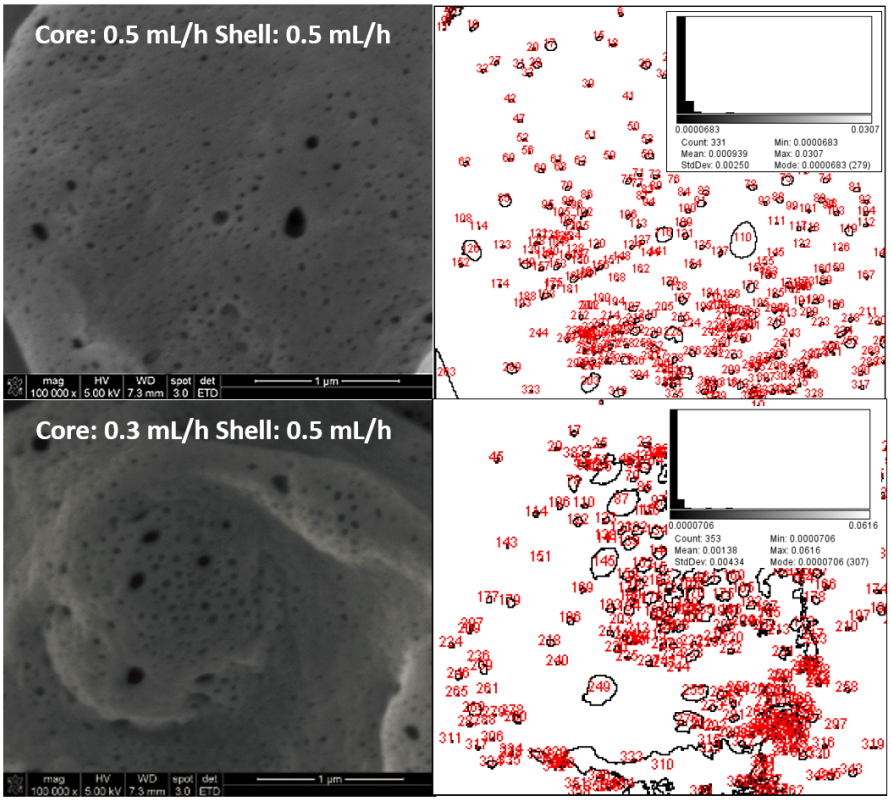

FIGURE 3.5: Area of Pores on Microparticle Shell Surface

The image on the right represents the corresponding threshold outline for the SEM image on the left. ImageJ converts the threshold into binary values and analyzes the pore area and distribution (histogram in the top right corner). The mean pore size for a core flow rate of 0.5 mL/h and 0.3 mL/h was about 0.00094 and 0.0014 um^2 respectively. It appears that at a slower core flow rate the pore size distribution is larger. At a lower core flow rate there is less material within the shell of the microparticle. The pores may have formed at a larger size at the lower flow rate due to the decrease in density of the microparticles; thus making it easier to form pores through the shell.

3.1.3 Agglomeration

Two type of solutions were made in order to compare the agglomeration of microparticles. Formulation A was the baseline solution used for normal testing and was compared to another solution that was the exact same solution excluding the addition of the Pluronic F-127. Figure 3.6 demonstrates the benefit of the addition of the dispersing agent in the shell solution.

The Fluorescent Microscope was used to image both solutions. Formulation A underwent proper pre- and post-processing methods while Formulation A - No Pluronic did not. It is clearly demonstrated that the sample with no pluronic developed a large agglomerate with many tiny particles attached to its surface. The image on the right shows properly dispersed microparticle throughout the solution.

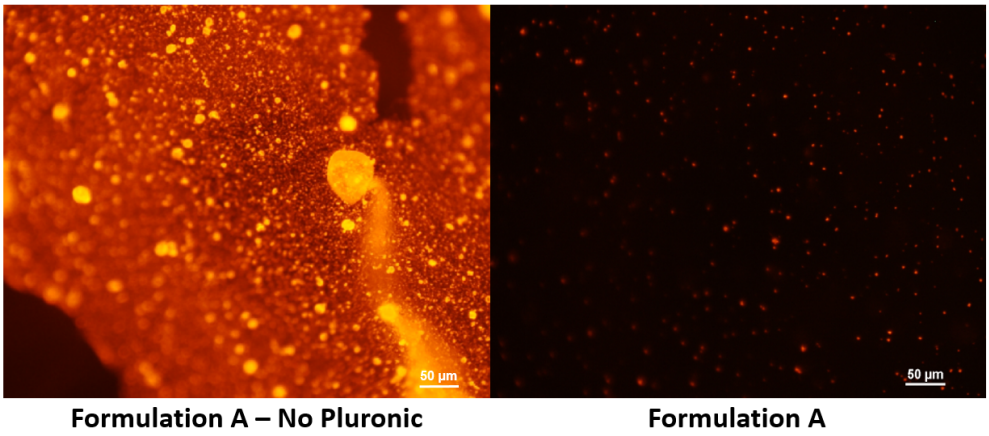

FIGURE 3.6: Comparison of Particles with and without Dispersing Agent

Figure 3.7 demonstrates the results from the sonication method. The image on the right was a sample prior to sonication; the sample on the left demonstrates the post-processing methods described in the previous chapter. The results indicate that the addition of the sonication post-treatment allows for the proper integration of the microparticles within the liquid in an attempt to form a more uniform solution.

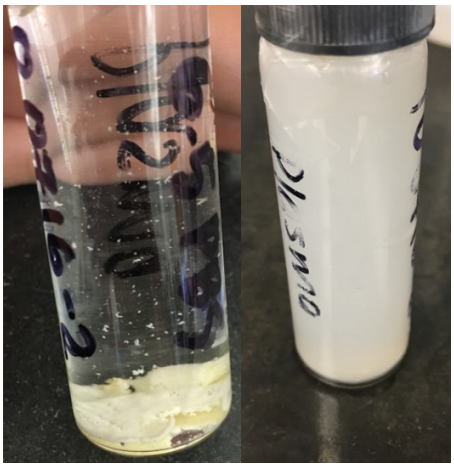

FIGURE 3.7: Sonicated Versus Unsonicated Sample

3.2 Leaching Design of Experiments

3.2.1 Percent Released

Samples were taken at time points: 1 day, 2 days, 7 days, 10 days, and 14 days. A calibration curve of fluorescent output versus various concentrations of Eosin Y in PBS was graphed in order to obtain a best fit trendline. The trendline was used to convert the fluorescent count of each time point to amount of dye released (mg). Comparing the amount released versus the initial dye amount, the percent released was then calculated. There appears to be some trend between various factors, but unfortunately the amount released for the DoE was not ideal. Figure 3.8 shows the amount released at each different factor. As it

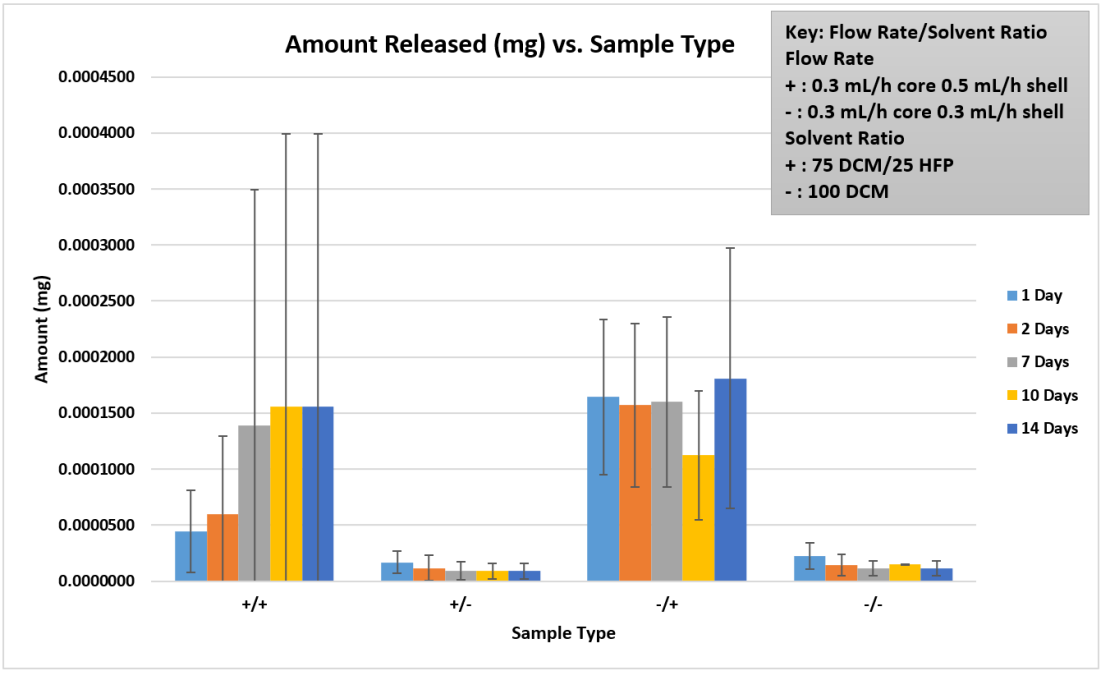

FIGURE 3.8: Amount Released (mg) Versus Sample Type

is shown the greatest amount of released dye was about 0.0001809 mg for sample type -/+ (Flow Rate/Solvent Ratio). It was hoped that over the period of 2 weeks there would have been a greater amount of dye released, but it can also been seen that there was a substantial amount of standard deviation between each of the replicates. The same observations can be shown for the percent released seen in Figure 3.9. The particles appear to only have released around

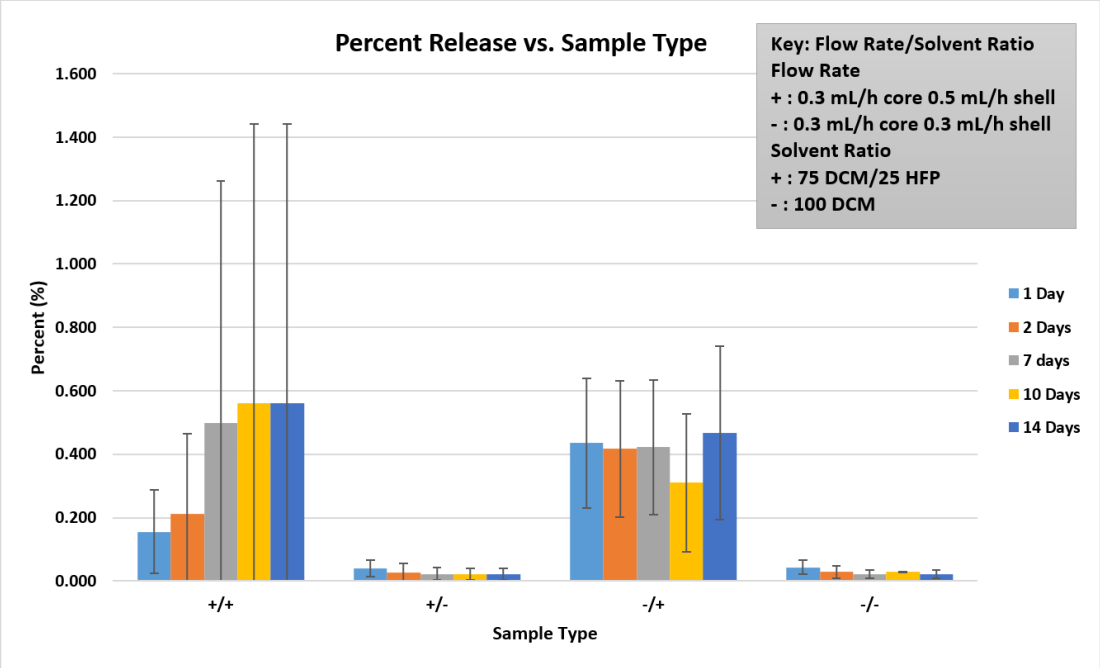

FIGURE 3.9: Percent Released (%) Versus Sample Type

0.56% and contain a large amount of standard deviation between the replicates. Since the microparticles are so small and the dye amount to be expected to be released is minimal given the relative initial amount there could be multiple sources of error. Since it took over a week to produce all the samples, the environment conditions (temperature, humidity) were not the same each day; potentially leading to slight deviations in morphology. Although it was not verified,

the dye could have had trouble diffusing through the ePTFE tubing. An SEM image was taken of the ePTFE tubing by itself to make sure there wasn't too large of pores, but maybe it didn't allow for the dye to diffuse enough and the dye remained "stuck" on the inner tubing. Just a small amount of dye "stuck" on the inner tubing would effect the proper analysis of simulated drug released because the experiment was dealing with such little amount of dye to begin. In order to improve this experiment it would be suggest to (1) simulate the drug diffusion through software to obtain theoretical values and (2) Use the data from the simulation to decide a new design of experiments that could potentially lead to data with less error.

The proof of concept test with the $Ru(dpp)_3Cl_2$ dye led to no detectable leaching for this experiment. Therefore, for reference, a graph from a prior study to this thesis involving $Ru(dpp)_3Cl_2$ was included below. It can be seen that there was

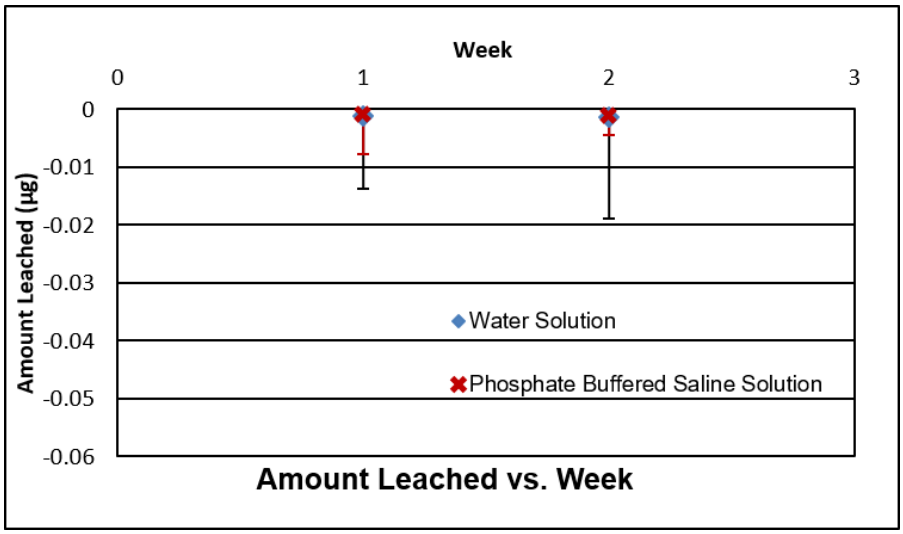

FIGURE 3.10: $Ru(dpp)_3Cl_2$ Released in PBS and Water

also negligible release data for this experiment.

3.2.2 JMP Statistical Analysis

A 2^2 Factorial design of experiments was performed in order to see the main affects and interactions between the various levels and factors. Using JMP Statistical Software, proper analysis was done in order to test if the percent of dye released was significantly different between each sample type. An example of the JMP ANOVA analysis is demonstrated below in Figure 3.11 A p-value of

Analysis of Variance

Source	DF	Sum of Squares	Mean Square	F Ratio
Model	3	0.30003166	0.100011	6.6835
Error	8	0.11971085	0.014964	Prob > F
C. Total	11	0.41974251		0.0143*

Parameter Estimates

Term	Estimate	Std Error	t Ratio	Prob>|t|
Intercept	0.1720818	0.035313	4.87	0.0012*
Flow Rate[0.3/0.3]	0.0739715	0.035313	2.09	0.0695
Solvent Ratio[100 DCM]	-0.123398	0.035313	-3.49	0.0081*
Solvent Ratio[100 DCM]*Flow Rate[0.3/0.3]	-0.065603	0.035313	-1.86	0.1003

Effect Tests

Source	Nparm	DF	Sum of Squares	F Ratio	Prob > F
Flow Rate	1	1	0.06566137	4.3880	0.0695
Solvent Ratio	1	1	0.18272501	12.2111	0.0081*
Solvent Ratio*Flow Rate	1	1	0.05164529	3.4513	0.1003

FIGURE 3.11: Day 1 ANOVA Statistics

0.0143 for the model was obtained. Therefore, at a significance level of 0.05, for day 1 leaching there is reason to believe that the new model is significantly better than the null. Analyzing the parameter estimates a flow rate p-value of 0.065 was obtained. At a significance level of 0.05 it is seen that there is no significant effect on percent released between the two levels. A p-value of 0.0081 for solvent

ratio, at a significance level of 0.05, indicates that there is significant different between solvent ratios on percent released. Lastly, the interaction between the two factors was observed. At a significance level of 0.05 a p-value of 0.1003 was obtained. Therefore there is no significant different between the interaction. In Figure 3.12 shows how the factor is significant. In Figure 3.13 it appears that

Level			Least Sq Mean
75/25 DCM/HFP	A		0.29547985
100 DCM		B	0.04868371

Levels not connected by same letter are significantly different.

FIGURE 3.12: Day 1 LSMeans Differences Student's t Solvent Ratio

Level	- Level	Difference	Std Err Dif	Lower CL	Upper CL	p-Value
75/25 DCM/HFP,0.3/0.3	100 DCM,0.3/0.5	0.3947391	0.0998794	0.164417	0.6250615	0.0042*
75/25 DCM/HFP,0.3/0.3	100 DCM,0.3/0.3	0.3780025	0.0998794	0.147680	0.6083249	0.0054*
75/25 DCM/HFP,0.3/0.3	75/25 DCM/HFP,0.3/0.5	0.2791493	0.0998794	0.048827	0.5094717	0.0234*
75/25 DCM/HFP,0.3/0.5	100 DCM,0.3/0.5	0.1155898	0.0998794	-0.114733	0.3459123	0.2805
75/25 DCM/HFP,0.3/0.5	100 DCM,0.3/0.3	0.0988532	0.0998794	-0.131469	0.3291756	0.3513
100 DCM,0.3/0.3	100 DCM,0.3/0.5	0.0167367	0.0998794	-0.213586	0.2470591	0.8711

FIGURE 3.13: Day 1 LSMeans Differences Student's t Solvent Ratio*Flow Rate

the first three interactions, at a signifance level of 0.05, is results in significantly different percent release. This is interesting due to the fact the the whole model test showed that there was not a significant difference with the interaction. This observation will be further explored at a future date with consultation on statistical interpretation.

Although the original graphs showed large standard deviations, for day 1 leaching data it appears that there are some significant results.

4 Discussion

4.1 Conclusion

The goal of this undergraduate research thesis was to first identify promising parameters that would aid in the development of optimal microparticle morphology. Once this goal was accomplished, the microparticles were to be analyzed in order to define guidelines for reproducible core-shell electrospraying fabrication.

From prior experimentation in the lab, agglomeration of microparticles was a known issue. A pre- and post-processing method was determined and from there optimal processing parameters were explored. Previous literature studies discussed how many different parameters could influence the microparticle morphology, such as solution flow rate, polymer concentration, solvent ratio, collection plate distance. Through Fluorescent Microscope imaging, it was determined that incorporation of a dispersing agent, plasma treatment of the glass storage vials, and sonication of the polymer solution would be necessary to rid the solution of particle agglomeration.

A baseline formulation, Formulation A, was used as a guideline for various solvent ratios and polymer concentrations. Formulation A was determined to

be the optimal solution parameters for oxygen sensing applications. The microparticles' morphology are typically spherical or cup-shape with limited fiber formation or porous shell surfaces. Through this experimentation another potential application was considered for this thesis: Drug Release. It was found that with the 100% DCM solvent mixture there was formation of pores on the particle shells. This could prove as a beneficial application for release of various types of drugs.

It was confirmed via SEM imaging that increasing the flow rate would increase the size of the microparticles. There also appeared to be a trend between collection distance and particle diameter where the farther the collection distance the larger the diameter. The DoE showed some significant results in regards to day 1 leaching data. There appears to be a significant effect on percent released given the solvent ratio. Also the interaction between solvent ratio and flow rate for certain factors provide significant results as well. It can be seen that there was significant different in percent released between the 75 DCM/25 HFP at 0.3 mL/h core and 0.3 mL/h shell and 100 percent DCM at 0.3 mL/h core and 0.3 mL/h shell. This can be justified by the SEM images. It was demonstrated that the 100 percent DCM resulted in pores while the 75/25 did not. It would make sense that the diffusion of the dye would be different given the microparticle morphology.

In summary, optimal processing parameters and formulations were determined for various biomedical applications. Results from analysis show that the best baseline solution for oxygen sensing capabilities is Formulation A. If drug

release application is of interest, it would be best to change the solvent ratio of Formulation A from 75 DCM : 25 HFP to 100% DCM in order to develop a porous shell. Since the greater the flow rate the more material gets pumped out of the needle tip, the optimal processing parameters was chosen based on the trade-off between production rate and particle quality. A 0.3 mL/h core and 0.5 mL/h shell proved to be an optimal processing parameter due to its spherical morphology and micro-sized particle diameter. A collection distance of 20 cm was chosen since it was a familiar distance used in the lab from previous studies, and provided a small enough particle for injectibility applications. It was necessary to develop a pre- and post-processing method in order to rid the solution of agglomeration. Therefore incorporation of the Pluronic F-127, plasma treated glass vial, and bath sonication treatment are all necessary in order to properly create a dispersed solution of core-shell microparticles. With combination of these findings and analysis, optimal core-shell microparticles can be developed and reproduced for applications in the biomedical field.

4.2 Contribution

This research aided in the development of creating reproducible core-shell electrosprayed microparticles for biomedical applications. It provides electrospraying processing parameters and pre and post-processing methods in order to

develop optimal microparticles. It provides evidence through Fluorescent Microscopy, SEM imaging, and Design of Experiments that correlates to other literature studies. With these findings, the lab will be able to manipulate the microparticles for further applications.

4.3 Future Work

With the completion of this research, the lab will be able to explore other areas of application or potential literary publication. If a drug release application should be of further interest, it would be best to explore another design of experiments regarding the leaching capabilities of the microparticles to try and obtain significant results. It may also be of interest to model the microparticles using software, such as COMSOL, in order to observe the theoretical diffusion of the dye from the core. Previous literature studies have demonstrated anywhere between 0% to 60% drug release [7]. In regards to the oxygen sensing application, the next step would be to incorporate the processing parameters defined above, with the development of the UCNPs into the polymer matrix. Once incorporated various alterations can be further explored by changing the location of the dye or making the core a liquid rather than a polymer. Another area of study would be to test the injectibility of these microparticle solutions in tissue phantoms to see their brightness capabilities *in vitro*.

A Design of Experiments for Leaching Study

The following images are the remaining days (2, 7, 10, and 14):

Response Response Time

Effect Summary

Summary of Fit

RSquare	0.58125
RSquare Adj	0.424219
Root Mean Square Error	0.166765
Mean of Response	0.171133
Observations (or Sum Wgts)	12

Analysis of Variance

Source	DF	Sum of Squares	Mean Square	F Ratio
Model	3	0.30882049	0.102940	3.7015
Error	8	0.22248343	0.027810	Prob > F
C. Total	11	0.53130393		0.0616

Parameter Estimates

Term	Estimate	Std Error	t Ratio	Prob>|t|
Intercept	0.1711332	0.048141	3.55	0.0075*
Solvent Ratio[100 DCM]	0.0514968	0.048141	1.07	0.3160
Flow Rate[0.3/0.3]	-0.143006	0.048141	-2.97	0.0179*
Solvent Ratio[100 DCM]*Flow Rate[0.3/0.3]	-0.051308	0.048141	-1.07	0.3176

LSMeans Differences Student's t

α= 0.050 t= 2.306

LSMean[j]

Mean[i]-Mean[j] / Std Err Dif / Lower CL Dif / Upper CL Dif		0.3/0.3	0.3/0.5
LSMean[i]	0.3/0.3	0	-0.286
		0	0.09628
		0	-0.508
		0	-0.064
	0.3/0.5	0.28601	0
		0.09628	0
		0.06399	0
		0.50804	0

Level		Least Sq Mean
0.3/0.5	A	0.31413890
0.3/0.3	B	0.02812753

Levels not connected by same letter are significantly different.

Level	- Level	Difference	Std Err Dif	Lower CL	Upper CL	p-Value
0.3/0.5	0.3/0.3	0.2860114	0.0962816	0.0639856	0.5080371	0.0179*

FIGURE A.1: Day 2 ANOVA Statistics

Response Response Time

Effect Summary

Summary of Fit

RSquare	0.318571
RSquare Adj	0.063035
Root Mean Square Error	0.396095
Mean of Response	0.241419
Observations (or Sum Wgts)	12

Analysis of Variance

Source	DF	Sum of Squares	Mean Square	F Ratio
Model	3	0.5867802	0.195593	1.2467
Error	8	1.2551323	0.156892	Prob > F
C. Total	11	1.8419125		0.3554

Parameter Estimates

Term	Estimate	Std Error	t Ratio	Prob>|t|
Intercept	0.2414194	0.114343	2.11	0.0677
Solvent Ratio[100 DCM]	-0.019539	0.114343	-0.17	0.8686
Flow Rate[0.3/0.3]	-0.219411	0.114343	-1.92	0.0913
Solvent Ratio[100 DCM]*Flow Rate[0.3/0.3]	0.0193804	0.114343	0.17	0.8696

FIGURE A.2: Day 7 ANOVA Statistics

Response Response Time

Effect Summary

Summary of Fit

RSquare	0.267561
RSquare Adj	-0.0071
Root Mean Square Error	0.453155
Mean of Response	0.230527
Observations (or Sum Wgts)	12

Analysis of Variance

Source	DF	Sum of Squares	Mean Square	F Ratio
Model	3	0.6001158	0.200039	0.9741
Error	8	1.6427927	0.205349	Prob > F
C. Total	11	2.2429085		0.4514

Parameter Estimates

Term	Estimate	Std Error	t Ratio	Prob>|t|
Intercept	0.2305269	0.130814	1.76	0.1160
Solvent Ratio[100 DCM]	-0.060656	0.130814	-0.46	0.6552
Flow Rate[0.3/0.3]	-0.205376	0.130814	-1.57	0.1551
Solvent Ratio[100 DCM]*Flow Rate[0.3/0.3]	0.0644288	0.130814	0.49	0.6356

FIGURE A.3: Day 10 ANOVA Statistics

Response Response Time

Effect Summary

Summary of Fit

RSquare	0.304115
RSquare Adj	0.043158
Root Mean Square Error	0.460707
Mean of Response	0.268116
Observations (or Sum Wgts)	12

Analysis of Variance

Source	DF	Sum of Squares	Mean Square	F Ratio
Model	3	0.7420613	0.247354	1.1654
Error	8	1.6980086	0.212251	Prob > F
C. Total	11	2.4400700		0.3813

Parameter Estimates

Term	Estimate	Std Error	t Ratio	Prob>|t|
Intercept	0.2681163	0.132995	2.02	0.0785
Solvent Ratio[100 DCM]	-0.023066	0.132995	-0.17	0.8666
Flow Rate[0.3/0.3]	-0.246502	0.132995	-1.85	0.1009
Solvent Ratio[100 DCM]*Flow Rate[0.3/0.3]	0.0233029	0.132995	0.18	0.8653

FIGURE A.4: Day 14 ANOVA Statistics

Bibliography

[1] Yutaka Amao. Probes and Polymers for Optical Sensing of Oxygen. *Microchimica Acta*, 143:1–12, September 2003.

[2] R.R. Anderson and J.A. Parrish. The Optics of Human Skin. *Journal of Investigative Dermatology*, 33:13–19, July 1981.

[3] N. Bock, T.R. Dargaville, and M.A. Woodruff. Electrospraying of Polymers with Therapeutic Molecules: State of the Art. *Progress in Polymer Science*, 3:1510–1551, November 2012.

[4] Seung-Woo Choi, Woo-Beom Choi, Yun-Hi Lee, Byeong-Kwon Ju, Man-Young Sung, and Byong-Ho Kim. The Analysis of Oxygen Plasma Pretreatment for Improving Anodic Bonding. *Journal of The Electrochemical Society*, 149:G8–G11, November 2001.

[5] National Center for Biotechnology Information.

[6] A. Jaworek, A. Krupa, M. Lackowski, A.T. Sobczyk, T. Czech, S. Ramakrishna, S. Sundarrajan, and D. Pliszka. Nanocomposite Fabric Formation by Electrospinning and Electrospraying Technologies. *Journal of Electrostatics*, 67:435–438, May 2009.

[7] Yi-Hsuan Lee, Fan Mei, Meng-Yi Bai, Suling Zhao, and Da-Ren Chen. Release Profile of Biodegradable-polymer-coated Drug Particles Fabricated by Dual-capillary Electrospray. *Journal of Controlled Release*, 145:58–64, March 2010.

[8] Lina Liu, Ruifei Qin, Haifeng Zhao, Xinguang Ren, and Zhongmin Su. Synthesis and Characterization of New Bifunctional Nanocomposites Processing Upconversion and Oxygen-sensing Properties. *Nanotechnology*, 28, June 2010.

[9] P. Moroshkin, P. Leiderer, Th. B. Moller, and K. Kono. Taylor Cone and Electrospraying at a Free Surface of Superfluid Helium Charged from Below. *Physical Review*, 95:1–9, May 2017.

[10] Chul Ho Park and Jonghwi Lee. Electrosprayed Polymer Particles: Effect of the Solvent Properties. *Journal of Applied Polymer Science*, 114:430–437, March 2009.

[11] Kayla F. Presley, Soshan Cheong, Alex Cochran, Richard D. Tilley, Josh E. Collins, and John J. Lannutti. Upconverter-powered Oxygen Sensing in Electrospun Polymeric Bilayers. *Sensors and Actuators B: Chemical*, 235:197–205, November 2016.

[12] Yiquan Wu, J. Andrew MacKay, Jonathan R. McDaniel, Ashutosh Chilkoti, and Robert L. Clark. Fabrication of Elastin-like Polypeptide Nanoparticles for Drug Delivery by Electrospraying. *Biomacromolecules*, 10:19–24, November 2009.

[13] Jingwei Xie and Chi-Hwa Wang. Encapsulation of Proteins in Biodegradable Polymeric Microparticles using Electrospray in the Taylor Cone-Jet Mode. *Biotechnology and Bioengineering*, 97:1278–1290, December 2007.

[14] R. Xue, M.T. Nelson, S.A. Teixeira, M.S. Viapiano, and J.J Lannutti. Cancer Cell Aggregate Hypoxia Visualized In vitro via Biocompatible Fiber Sensors. *Biomaterials*, 76:208–217, January 2016.

[15] Ruipeng Xue, Prajna Behera, Mariano S. Viapiano, and John J. Lannutti. Rapid Response Oxygen Sensing Nanofibers. *Materials Science and Engineering*, 33:3450–3457, August 2013.

[16] L. Zhang, J. Huang, T. SI, and R.X. Xu. Coaxial Electrospray of Microparticles and Nanoparticles for Biomedical Applications. *Expert Review of Medical Devices*, 9:595–612, November 2012.

[17] Susan Y Zhao and Benjamin S Harrison. Morphology Impact on Oxygen Sensing Ability of Ru(dpp)3Cl2 Containing Biocompatible Polymers. *Materials Science and Engineering*, 53:280–285, August 2015.